Hindawi Publishing Corporation
International Journal of Photoenergy
Volume 2014, Article ID 589027, 7 pages
http://dx.doi.org/10.1155/2014/589027

Research Article

Postdeposition Annealing Effect on Cu_2ZnSnS_4 Thin Films Grown at Different Substrate Temperature

Samia Ahmed Nadi,[1] Puvaneswaran Chelvanathan,[1] Zaihasraf Zakaria,[1] Mohammad Mezbaul Alam,[2] Zeid A. Alothman,[2] Kamaruzzaman Sopian,[1] and Nowshad Amin[1,2,3]

[1] *Solar Energy Research Institute (SERI), Universiti Kebangsaan Malaysia, 43600 Bangi, Selangor, Malaysia*
[2] *Advanced Materials Research Chair (AMRC), Chemistry Department, College of Sciences, King Saud University, Riyadh 11451, Saudi Arabia*
[3] *Department of Electrical, Electronic and Systems Engineering, Universiti Kebangsaan Malaysia, 43600 Bangi, Selangor, Malaysia*

Correspondence should be addressed to Nowshad Amin; nowshad@eng.ukm.my

Received 26 January 2014; Revised 15 March 2014; Accepted 17 March 2014; Published 29 April 2014

Academic Editor: Raghu N. Bhattacharya

Cu_2ZnSnS_4 (CZTS) thin films were deposited on top of Molybdenum (Mo) coated soda lime glass (SLG) substrates using a single target rf magnetron sputtering technique. The sputtering parameters such as base pressure, working pressure, rf power, argon (Ar) gas flow rate, and deposition time were kept consistent throughout the experiment. The effect of different substrate temperatures, for example, room temperature (RT), 300°C, 350°C, 370°C, 400°C, and 450°C, was analyzed by studying their structural, electrical, and optical properties. As-sputtered films were then annealed at 460°C. X-ray diffraction (XRD) measurement revealed the structure to be kesterite with peak of (112) plane in both annealed and as-sputtered CZTS thin films. The crystallinity of the films improved with the increasing substrate temperature until 370°C. Secondary phases of MoS_2, Cu_xMoS_x, Cu_xSnS_x, Cu_xS, and Cu_6MoSnS_8 (hemusite) were also observed in the annealed CZTS films. Scanning electron microscopy (SEM) shows crystallite size of deposited CZTS thin film to be proportionally related to deposition temperature. The highest surface roughness of 67.318 nm is observed by atomic force microscopy (AFM). The conductivity type of the films was found to be p-type by Hall effect measurement system.

1. Introduction

Solar photovoltaic is rapidly becoming the leading choice as a clean electricity generation method. This is due to its intrinsic nature of requiring no fuel, being silent, and releasing no by-product gases into the environment whereas conventional electricity generation method like fossil fuel combustion creates pollution by exhausting gases such as CO_2, NO_2, CO, and SO_2 into the environment. PV industry has experienced a significant increase in progress both in terms of scientific breakthrough and commercialization success in the past years due to the desire of world community to decrease their dependence on fossil fuel driven electricity generation. To date single and multicrystalline silicon technology has dominated the PV market due to its proven performance stability and high effectiveness module over the years [1]. However, due to high energy consumption processes which are involved in Silicon PV, scientific community has set their effort towards an alternative technology of thin film solar cells (TFSC). TFSC has the potential to be less expensive for its low material usage and low temperature processing methods. Furthermore, TFSC can be fabricated by various types of deposition methods on low cost rigid as well as flexible substrates [2]. Among the thin film solar cells, particularly $CuIn_xGa_{1-x}(S, Se)_2$ (CIGSSe), $CuInSe_2$ (CIS) and CdTe are already being commercialized for large scale PV manufacturing. $Cu(In_xGa_{1-x})Se_2$ (CIGS) already achieved a record efficiency of 20.4% [1, 2]. However, CIGS and CdTe solar cell devices contain elements such as indium (In), selenium (Se), and tellurium (Te) which are rare in the earth's crust (indium and selenium are merely 0.05 ppm or less) and toxic [3]. Due to the imperative need of environmentally

Table 1: Parameters of Mo sputtering.

Parameters	Value
Base pressure	8.1×10^{-5} Torr
Working pressure	3.6×10^{-2} Torr
Ar flow rate	9 SCCM
RF power	125 Watt
Substrate temperature	RT

Table 2: Parameters of CZTS deposition.

Parameters	Value
Base pressure	3.5×10^{-5} Torr
Working pressure	3.6×10^{-2} Torr
Ar flow rate	10 SCCM
RF power	30 Watt
Time	180 minutes

benign solar cells, Cu_2ZnSnS_4 (CZTS) absorber thin film has recently drawn attention in the photovoltaic (PV) research field. The elements of this new absorber material of I_2-II-IV-VI_4 CZTS consist of Cu (50 ppm), Zn (75 ppm), Sn (2.2 ppm), and S (260 ppm) which are relatively abundant and nontoxic [4]. CZTS possesses Kesterite crystal structure [5] and it is a p-type semiconductor which has a suitable band gap energy in the range of of 1.4-1.5 eV and large absorption coefficient over $10^4\,cm^{-1}$ [6–8]. Despite these interesting optical properties, so far a conversion efficiency of 12.6% has been achieved using a CZTSSe absorber layer by hydrazine chemical process [9]. Due to the aforesaid selenium scarcity and toxicity, pure sulfide based CZTS device is preferred rather than pure selenide or mixed sulfur-selenium containing device. Furthermore, physical vapor deposition method is more favorable than chemical process (hydrazine based process [10], electrodeposition [11], and sol-gel deposited [12]) due to ease of scalability and compatibility in large scale commercialization manufacturing plant. Shin et al. reported highest efficiency of 8.4% for pure sulfide CZTS thin film solar cells fabricated by thermal evaporation method [13]. Efficiency more than 10% in laboratory scale is imperative for research start-up of mini submodules and subsequent large modules. Another popular route for CZTS polycrystalline deposition is sputtering of precursor followed by postdeposition heat treatment to promote crystal growth [14]. Sputtered precursor may consist of only metallic elements (Cu-Zn-Sn) or sulfur containing compound (Cu(S)-Zn(S)-Sn(S)) in which the nature of initial precursor properties will dictate the final CZTS absorber layer properties (elemental composition, crystal structure, surface morphology, electrical resistivity, and optical properties) after the heat treatment process. However CZTS material suffers from secondary phase formation rather easily due to the narrow window of thermodynamically stable phase [15]. Hence, incomplete intermixing of sputtered precursor during heat treatment can yield substantial undesired binary and ternary phases which can be detrimental in complete device.

In this study, sputtering of single stoichiometric quaternary target of CZTS has been carried by RF sputtering system. Substrate temperature during film growth has been varied from room temperature to 450°C while other process variables fixed. Finally, the sputtered films underwent heat treatment. The aim of this study can be divided into 2 aspects. Firstly, the effects of substrate temperature on as-sputtered films were the primary concern in this investigation. Hence, crystal structure, elemental composition, and surface morphology evolution of CZTS with respect of substrate temperature were analyzed. Secondly, the property changes incurred to the as-sputtered films after the heat treatment were studied. In order to quantitatively analyze the substrate temperature effect as well as the heat treatment induced alteration in the film, film crystallinity, grain size, elemental composition, and surface roughness were probed by various methods and the results are presented herein.

2. Experiment

2.1. Deposition Conditions. CZTS thin films were deposited on Mo coated soda lime glass substrates of 75 mm × 25 mm × 1 mm by radio frequency (RF) magnetron sputtering system. Prior to deposition, all the substrates were cleaned ultrasonically in methanol (Sigma Aldrich)-acetone (Sigma Aldrich)-methanol-deionised water sequence and finally dried by blowing N_2 gas. Molybdenum (50.8 mm diameter, 99.95% purity, Kurt. J. Lesker) back contact was also sputtered by RF sputtering mechanism with the process variable as shown in Table 1. With the mentioned sputtering deposition condition, a 1.6 μm thick Mo was achieved. Source material for CZTS absorber layer used in this study is a 50.8 mm diameter stoichiometric (Cu: 25%, Zn: 12.5%, Sn; 12.5% and S: 50%) CZTS (Mitsui Ltd. purity: 99.99%) sputtering target.

CZTS deposition condition is shown in Table 2. Different substrate temperatures such as RT, 300°C, 350°C, 370°C, 400°C, and 450°C were investigated. All samples were cooled down naturally after the sputtering process before they were taken out to avoid oxidation.

Structural and crystallinity properties as well as the deposited film orientation along the film's surface normal were examined by BRUKER aXS-D8 Advance Cu-Kα diffractometer. XRD patterns were recorded in the 2θ range from 10° to 80° using Cu Kα radiation wavelength, λ = 1.5408 Å. Grain size, surface morphology, and compositional analysis were observed by using SUPRA 55 VP field emission scanning electron microscope (FESEM) equipped with energy dispersive X-ray (EDX) capabilities. EDX measurements were at operating voltage of 15 kV and effective spot size of 1 μm. Surface topography and roughness were analyzed by using nano surf atomic force microscope (AFM) with noncontact mode settings.

2.2. Postdeposition Parameters

2.2.1. CZTS Annealing Process. The as-sputtered SLG/Mo/CZTS thin films were annealed in vacuum condition in an electric furnace heated up to 460°C. Using rotary vacuum

Table 3: Deposition condition of the CZTS absorber layer.

Temperature	As sputtered films	Annealed films
RT	A1	B1
300°C	A2	B2
350°C	A3	B3
370°C	A4	B4
400°C	A5	B5
450°C	A6	B6

pump and N_2 gas; the undesired air was purged from the quartz tube several times before final vacuum evacuation. The samples were placed in alumina crucible which was precleaned ultrasonically with methanol and acetone to remove contaminant particles. Temperature of the tube furnace was increased from room temperature to 460°C with constant ramp-up rate of 25°C/min. Effective holding time was 60 minutes, followed by natural cooling process with the heater lid closed. The annealing profile (temperature versus time) is depicted in Figure 1.

2.2.2. Sample Identification. The as-sputtered samples were denoted by A (A1–A6) and the annealed samples by B (B1–B6). (see Table 3).

3. Results and Discussion

3.1. The Effects of Substrate Temperature on As-Sputtered Film. In our related works, we have found that the as-sputtered films prepared at 370°C exhibited strong preferential orientation of (112) plane, better crystallinity, and larger grain sizes than the other films sputtered at substrate temperature of 300°C, 350°C, 370°C, 400°C, and 450°C [16]. In this experiment, we added CZTS thin films prepared at room temperature (RT) to investigate the effects on the properties followed by postdeposition annealing treatment of all the films.

3.2. Structural and Compositional Studies. To examine the influence of substrate deposition temperature, the crystallographic properties of as-deposited CZTS films were characterized by XRD and their patterns are shown in Figures 2 and 3. As-sputtered films deposited at 350°C and above exhibit preferential CZTS crystal orientation of (112) from XRD measurement whereas film sputtered below 350°C did not show any significant peak other than Mo. This may serve as an indication that nucleation of sputtered CZTS starts at onset temperature of 350°C. Increase in substrate temperature from RT to 370°C improves the crystallinity of CZTS films as revealed by the increasing peak intensity. The samples A1, A2, A3, A4, A5, and A6 showed highest (112) diffraction peak at 2θ = 28.48°, 28.52°, 28.52°, 28.60°, 28.56°, and 28.60°, respectively, indicating the formation of kesterite type CZTS thin film (JCPDS 26-0575). Here, sample A4 showed more pronounced peak intensity than the other samples, indicating optimum growth temperature of CZTS thin film. The crystallinity decreases for films deposited at higher than

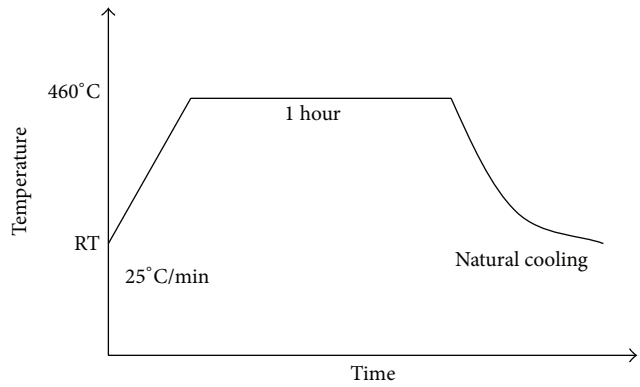

Figure 1: Temperature profile for annealing treatment.

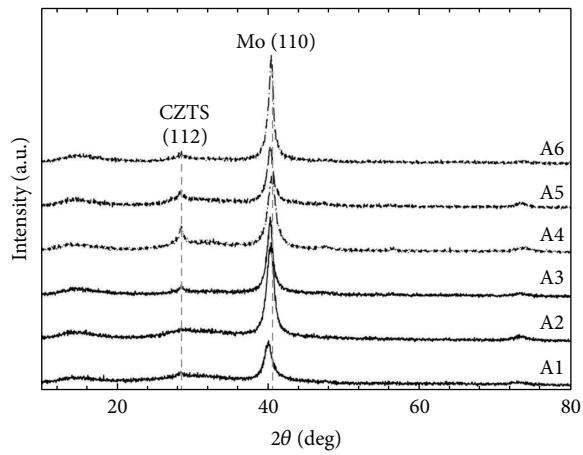

Figure 2: X-ray diffraction patterns of the as-sputtered CZTS films grown at various substrate temperatures.

370°C for samples A5 and A6. By scrutinizing the EDX result in Figure 4, sample A4 has the closest atomic ratio for a stoichiometric CZTS structure. Other samples exhibit severe Zn loss and excess of S (with respect to target's elemental composition supplied by manufacturer). This is consistent with findings from Xie et al. [17] whereby Zn loss occurs during single ceramic target sputtering. Zn loss is attributed to the high partial pressure of Zn combined with the elevated temperature during sputtering which facilitates Zn migration out of CZTS film. No elemental Zn diffraction peak was detected, ruling out the possibility of Zn dissociation from CZTS crystal and segregation in CZTS films. Since no external sulfur was supplied during annealing, increase in sulfur can be attributed to the normalization effect of elements from EDX measurement. Under this condition, formation of SnS compound is most likely to happen although no SnS peak was detected in the XRD spectra. Diffraction peak of Mo could also be observed due to the Mo substrate.

In order to optimize the growth condition of CZTS due to annealing treatment Figure, 3 shows the XRD patterns of the annealed CZTS films obtained at different substrate temperature. Here, the CZTS diffraction peaks of (112) were seen for samples B1, B2, B3, B4, and B5 at 2θ = 28.56°,

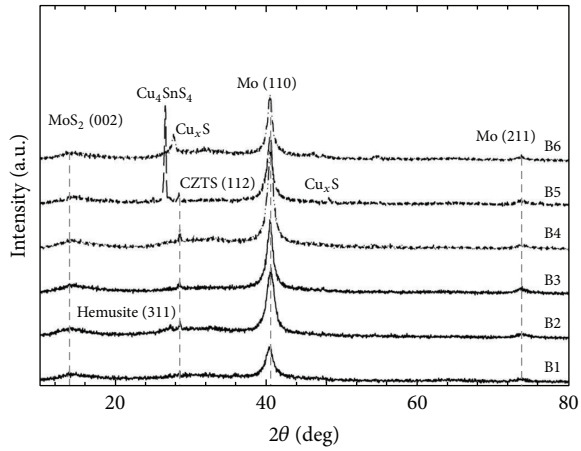

Figure 3: X-ray diffraction patterns of the annealed CZTS films grown at various substrate temperatures.

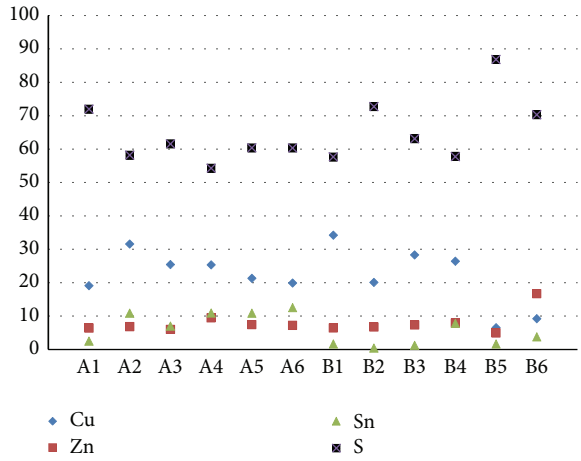

Figure 4: Atomic concentration from energy dispersive X-ray analysis (EDX).

28.56°, 28.52°, 28.56°, and 28.44°, respectively. Sample B6 did not show any dominating CZTS peak. Some secondary phases such as MoS_2 (002), hemusite (Cu_6MoSnS_8) (311), Cu_4SnS_4 (102), and Cu_2S (103) could be observed as a polycrystalline nature [7, 18, 19]. The secondary phase of MoS_2 could be observed at $2\theta = 13.88°$, 13.84°, 14.20°, 14.28°, and 14.32° for samples B2, B3, B4, B5, and B6, respectively. All annealed films show severe Sn loss which can be attributed to the high partial pressure of SnS and Sn compound and element, respectively [20]. Combined with Zn loss in the initial precursors and compounded by the Sn loss after the annealing process, formation of secondary phase is expected. Formation of Cu_6MoSnS_8 and MoS_2 compounds indicate interdiffusion of Mo and CZTS compound due to the additional thermal energy, whereas the peak of hemusite could be seen at 26.76° on the sample B3. This finding is consistent with the report from Scragg et al. group whereby they have found secondary phase formation at the back contact during annealing [21]. At about $2\theta = 26.64°$ and 47.2°, peak of Cu_4SnS_4 and Cu_2S could be observed for sample B6. The presence of secondary phase may arise from the excess Cu and poor Zn. From Figure 3, it can be signified that Cu_2S or Cu_xSnS_x do not form compounds at low temperature [22]. Sample B5 exhibited a Cu-Sn sulphide peak whereas sample B6 showed no formation of Sn. It is thought that at 450°C substrate temperature, Sn was extremely deficient and Cu could not react easily with Sn. Comparable outcomes that copper-rich impurity phase also easily occurred in Cu-rich CZTS thin film had been reported by other researchers [23, 24]. However, drastic increase of Zn concentration in sample B6 was not anticipated given that a steady trend of Zn loss has been already observed for all the samples (as-sputtered and annealed). Hence, this anomaly is subject for further studies; however, initial assumption for this phenomenon is that the concentration variation is positional dependent meaning that the EDX spot might have probed ZnS compound giving rise to Zn and S elemental ratio.

From the XRD patterns some secondary phases could be observed on the annealed films. For sample B2, hemusite (Cu_6MoSnS_8) might have occurred due to extreme Zn deficiency which can be explained by the EDX spectroscopy results. With the elevation of substrate temperature, the secondary phase forms until it reached higher temperature of 400°C and the CZTS film started decomposing.

3.3. Topological and Morphological Properties. Surface topology studies were performed by AFM measurement and are shown in Figure 5. RMS surface roughness and surface morphology were analyzed and the surface roughness trend is plotted in Figure 6. As-sputtered films show relatively lower surface roughness compared to annealed films. Higher roughness values of annealed films are attributed to larger grain size due to better nucleation process during annealing process. Larger grain clusters are confirmed by the surface topology attained from AFM and also the measured grain size from FESEM images as showed in Figure 10.

From the AFM images in Figure 6, the difference in the topology of two samples, sample A4 and sample B4, can be well observed. It can be seen that sample A4 has smaller grain size and more pinholes. Whereas because of annealing treatment of the same sample, the grain size increased, as well as the fact that pinholes were eliminated.

Substrate temperature affects the morphology of CZTS thin films by influencing the growth rate of the nanocrystals. For the as-sputtered films, sample A4 has the highest grain size of 191.05 nm. Annealing of A4 film which is sample B4 showed increased grain size of 215.94 nm which is the highest grain size achieved in this experiment. From Figure 7, it can be clearly discerned that an important structural property that was affected due to annealing treatment is the grain size. Decrease in grain size for samples sputtered at 400°C and 450°C is in agreement with the XRD spectra in which CZTS peaks are not detected.

Figure 8(a) shows cross-sectional view of FESEM images of the A4 which recorded highest crystallinity and grain size. Figure 8(b) depicts the view of B4 which also exhibited highest crystallinity, highest grain size, and no secondary phases.

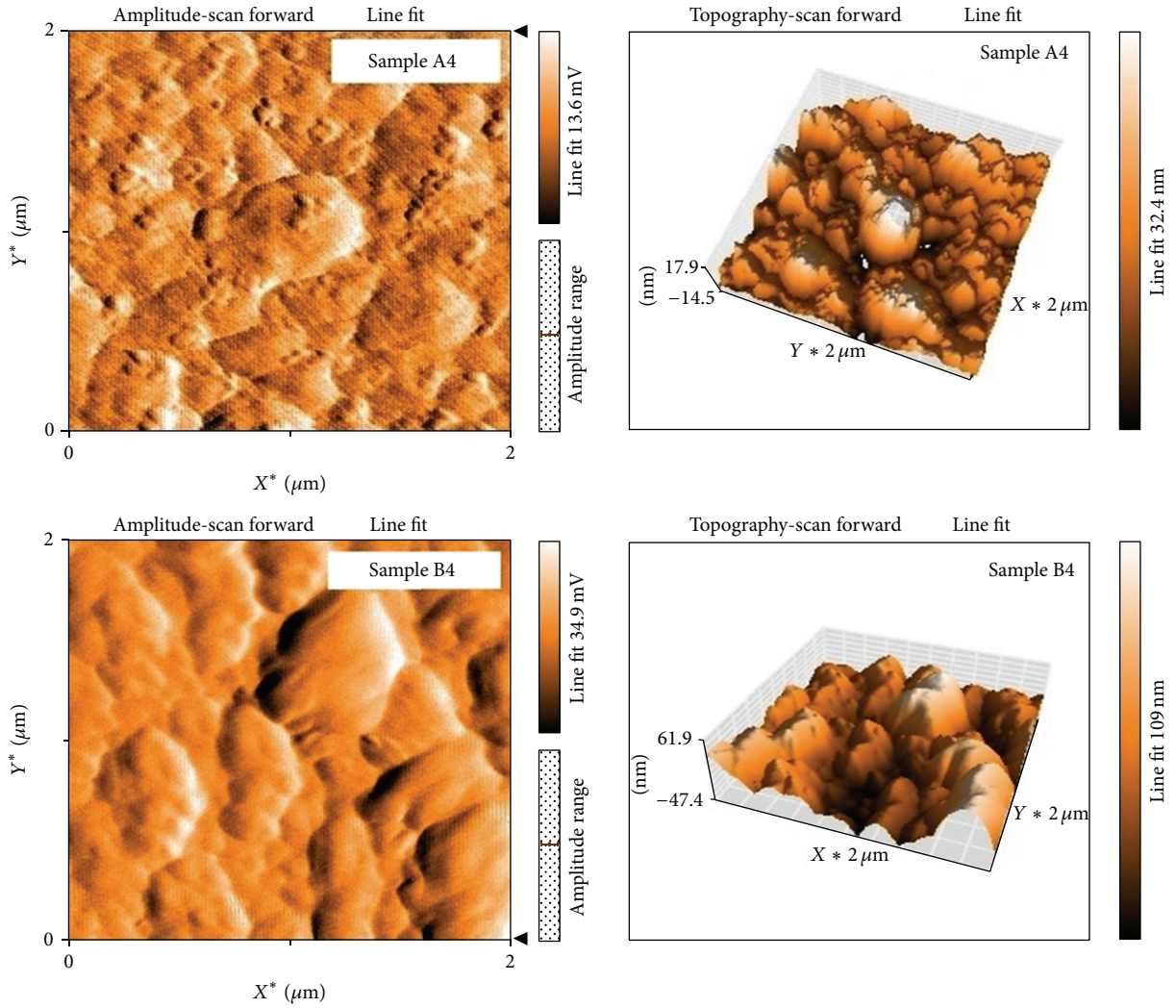

Figure 5: Surface morphology of sample A4 (grown at 370°C) and B4 (annealed at 460°C).

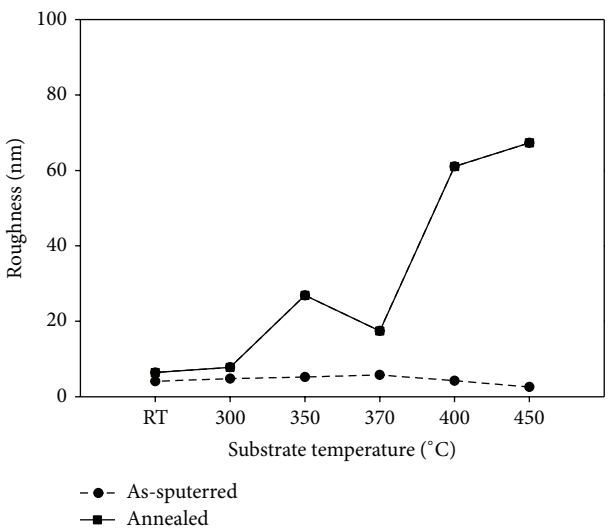

Figure 6: Surface roughness of as-sputtered and annealed films analyzed by AFM measurement.

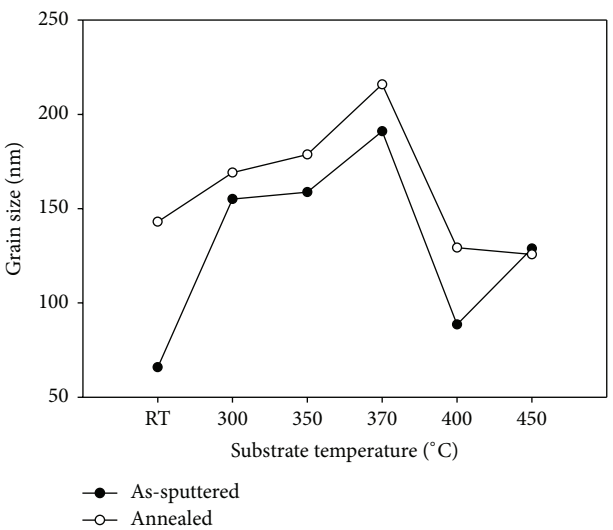

Figure 7: Improvement in crystallite size of as-sputtered and annealed films from SEM measurement.

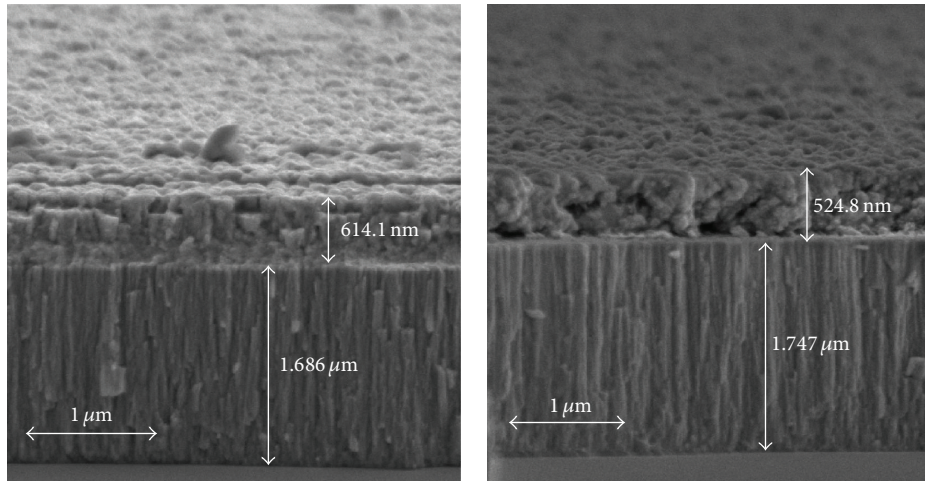

Figure 8: Cross-sectional view of sample A4 (grown at 370°C) and B4 (annealed and grown at 460°C) observed by SEM.

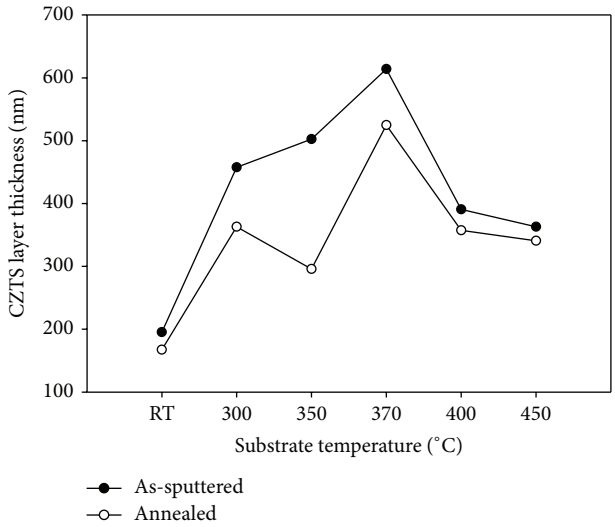

Figure 9: Thickness variation of as-sputtered and annealed CZTS films.

Significant changes could be observed on the thickness of CZTS films. Although all the deposition parameters were the same except the substrate temperature, for as-sputtered films, with the increase of substrate temperature the thickness of CZTS film increased up to 370°C substrate temperature from 65.9 nm (at RT) to 191.05 nm (at 370°C) and then it started decreasing. The annealed films followed the same trend as from thickness of A1 = 195.4 nm (at RT) to B4 = 614.1 nm at 370°C. But due to the annealing treatment, the thickness of the films decrease than that of the as-sputtered films fabricated at the same substrate temperature. Figure 9 illustrates the variation of the thickness of CZTS films (as-sputtered and annealed) more specifically. Lower thickness of annealed films is due to rearrangement of CZTS lattice due to thermal agitation during annealing process. Hence, CZTS film densifies and becomes more compact consequently decreasing the film thickness.

The morphology of the annealed CZTS films showed some voids (Figure 10(a)) at lower substrate temperature that disappeared with the increase of the substrate temperature. Sample B4 showed no voids and highest grain size which can be observed from Figure 10(b). Fewer voids in the CZTS absorber layer are desirable as it leads to higher conversion efficiency [10].

4. Conclusion

CZTS thin films were sputtered at 6 different substrate temperatures ranging from room temperature to 450°C and subsequently vacuum annealed for 60 minutes at 460°C. Structural analysis for as-sputtered films showed that substrate temperature of 370°C results in the highest crystallinity, grain size, and layer thickness. This trend is attributed to the atomic ratio of the film which was the closest to the stoichiometric CZTS compound confirmed by EDX measurement. Surface roughness of as-sputtered films was insensitive to substrate temperature as minimal variation of RMS roughness was found but undesirable pinholes were observed. As for annealed films, the thickness decreased due to heat treatment which densified the as-sputtered precursors. However, larger grains were detected confirming that annealing process induces better nucleation and grain coalescence upon recrystallization. Annealed films possess rougher surface for CZTS films grown at 370°C and subsequently annealed at 460°C, which demonstrate the lowest roughness, suitable for application to photovoltaic absorber layer.

Conflict of Interests

The authors declare that there is no conflict of interests regarding the publication of this paper.

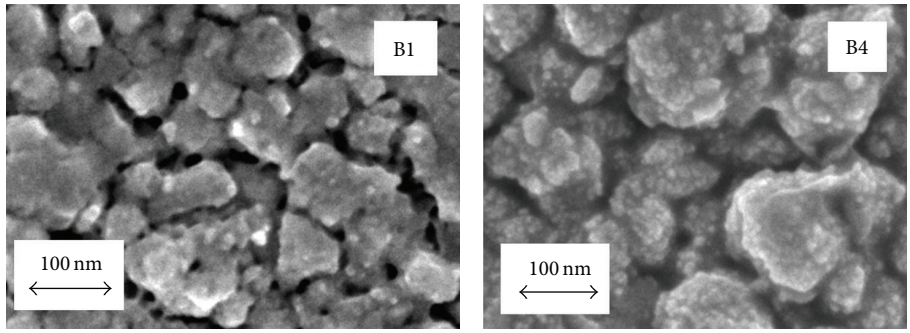

Figure 10: Surface morphology of sample B1 (as-grown) and B4 (annealed at 370°C).

Acknowledgments

This project was supported by King Saud University, Deanship of Scientific Research, College of Science Research Center.

References

[1] P. Jackson, D. Hariskos, E. Lotter et al., "New world record efficiency for Cu(In,Ga)Se_2 thin-film solar cells beyond 20%," *Progress in Photovoltaics: Research and Applications*, vol. 19, no. 7, pp. 894–897, 2011.

[2] http://www.empa.ch/plugin/template/empa/*/131441.

[3] C. Wadia, A. P. Alivisatos, and D. M. Kammen, "Materials availability expands the opportunity for large-scale photovoltaics deployment," *Environmental Science and Technology*, vol. 43, no. 6, pp. 2072–2077, 2009.

[4] J. Emsley, *The Elements*, Oxford University Press, Oxford, UK, 3rd edition, 1998.

[5] JCPDS (Joint Committee on Powder Diffraction Standards) card 26 575.

[6] J. M. Raulot, C. Domain, and J. F. Guillemoles, "Ab initio investigation of potential indium and gallium free chalcopyrite compounds for photovoltaic application," *Journal of Physicsand Chemistry of Solids*, vol. 66, pp. 2019–2023, 2005.

[7] P. A. Fernandes, P. M. P. Salomé, and A. F. da Cunha, "Cu_xSnS_{x+1} (x = 2, 3) thin films grown by sulfurization of metallic precursors deposited by dc magnetron sputtering," *Physica Status Solidi C: Current Topics in Solid State Physics*, vol. 7, no. 3-4, pp. 901–904, 2010.

[8] J. P. Leitão, N. M. Santos, P. A. Fernandes et al., "Study of optical and structural properties of Cu_2ZnSnS_4 thin films," *Thin Solid Films*, vol. 519, pp. 7390–7393, 2011.

[9] W. Wang, M. T. Winkler, O. Gunawan et al., "Device characteristics of CZTSSe thin-film solar cells with 12.6% efficiency," *Advanced Energy Materials*, 2013.

[10] T. K. Todorov, K. B. Reuter, and D. B. Mitzi, "High-efficiency solar cellwith earth-abundant liquid-processed absorber," *Advanced Materials*, vol. 22, no. 20, pp. E156–E159, 2010.

[11] A. Ennaoui, M. Lux-Steiner, A. Weber et al., "Cu_2ZnSnS_4 thin film solar cells from electroplated precursors: novel low-cost perspective," *Thin Solid Films*, vol. 517, no. 7, pp. 2511–2514, 2009.

[12] K. Tanaka, N. Moritake, and H. Uchiki, "Preparation of Cu_2ZnSnS_4 thin films by sulfurizing sol-gel deposited precursors," *Solar Energy Materials and Solar Cells*, vol. 91, no. 13, pp. 1199–1201, 2007.

[13] B. Shin, O. Gunawan, Y. Zhu, N. A. Bojarczuk, S. Jay Chey, and S. Guha, "Thin film solar cell with 8.4% power conversion efficiency using an earth-abundant Cu_2ZnSnS_4 absorber," *Progress in Photovoltaics: Research and Applications*, vol. 21, no. 1, pp. 72–76, 2011.

[14] J. J. Scragg, T. Ericson, X. Fontané et al., "Rapid annealing of reactively sputtered precursors for Cu_2ZnSnS_4 solar cells," *Progress in Photovoltaics: Research and Applications*, vol. 22, no. 1, pp. 10–17, 2014.

[15] S. Chen, J.-H. Yang, X. G. Gong, A. Walsh, and S.-H. Wei, "Intrinsic point defects and complexes in the quaternary kesterite semiconductor Cu_2ZnSnS_4," *Physical Review B: Condensed Matter and Materials Physics*, vol. 81, no. 24, Article ID 245204, 2010.

[16] S. A. Nadi, P. Chelvanathan, M. M. Alam et al., "Effect of substrate temperature on the growth of CZTS thin films by RF magnetron sputtering," in *Proceedings of the IEEE Conference on Clean Energy and Technology (CEAT '13)*, pp. 466–468, 2013.

[17] M. Xie, D. Zhuang, M. Zhao, B. Li, M. Cao, and J. Song, "Fabrication of Cu_2ZnSnS_4 thin films using a ceramic quaternary target," *Vacuum*, vol. 101, pp. 146–150, 2014.

[18] H. Wang, "Progress in thin film solar cells based on Cu_2ZnSnS_4," *International Journal of Photoenergy*, vol. 2011, Article ID 801292, 10 pages, 2011.

[19] P. A. Fernandes, P. M. P. Salomé, and A. F. daCunha, "Growth and Raman scattering characterization of Cu_2ZnSnS_4 thin films," *Thin Solid Films*, vol. 517, pp. 2519–2523, 2009.

[20] S. Schorr, A. Weber, V. Honkimäki, and H. W. Schock, "In-situ investigation of the kesterite formation from binary and ternary sulphides," *Thin Solid Films*, vol. 517, pp. 2461–2464, 2009.

[21] J. J. Scragg, J. T. Wätjen, M. Edoff, T. Ericson, T. Kubart, and C. Platzer-Björkman, "A detrimental reaction at the molybdenum backcontact in $Cu_2ZnSn(S, Se)_4$ thin-film solar cells," *Journal of the American Chemical Society*, vol. 134, pp. 19330–19333, 2012.

[22] I. D. Olekseyuk, I. V. Dudchak, and L. V. Piskach, "Phase equilibria in the Cu_2S-ZnS-SnS_2 system," *Journal of Alloys and Compounds*, vol. 368, no. 1-2, pp. 135–143, 2004.

[23] L. Sun, J. He, H. Kong, F. Yue, P. Yang, and J. Chu, "Structure, composition and optical properties of Cu_2ZnSnS_4 thin films deposited by Pulsed Laser Deposition method," *Solar Energy Materials and Solar Cells*, vol. 95, no. 10, pp. 2907–2913, 2011.

[24] H. Yoo and J. Kim, "Growth of Cu_2ZnSnS_4 thin films using sulfurization of stacked metallic films," *Thin Solid Films*, vol. 518, no. 22, pp. 6567–6572, 2010.